Article

Cell
PRESS

PRG-1 and 21U-RNAs Interact to Form the piRNA Complex Required for Fertility in *C. elegans*

Pedro J. Batista,[1,5,10] J. Graham Ruby,[2,3,6,10] Julie M. Claycomb,[1] Rosaria Chiang,[2,3,6] Noah Fahlgren,[7,8] Kristin D. Kasschau,[7,8] Daniel A. Chaves,[1] Weifeng Gu,[1] Jessica J. Vasale,[1] Shenghua Duan,[1] Darryl Conte, Jr.,[1] Shujun Luo,[9] Gary P. Schroth,[9] James C. Carrington,[7,8] David P. Bartel,[2,3,6,*] and Craig C. Mello[1,4,*]
[1]Program in Molecular Medicine, University of Massachusetts Medical School, Worcester, MA 01605, USA
[2]Howard Hughes Medical Institute
[3]Department of Biology
Massachusetts Institute of Technology, Cambridge, MA 02139, USA
[4]Howard Hughes Medical Institute, Worcester, MA 01605, USA
[5]Gulbenkian PhD Programme in Biomedicine, Rua da Quinta Grande, 6, 2780-156, Oeiras, Portugal
[6]Whitehead Institute for Biomedical Research, 9 Cambridge Center, Cambridge, MA 02142, USA
[7]Center for Gene Research and Biotechnology
[8]Department of Botany and Plant Pathology
Oregon State University, Corvallis, OR 97331, USA
[9]Illumina, Inc., Hayward, CA 94545, USA
[10]These authors contributed equally to this work
*Correspondence: dbartel@wi.mit.edu (D.P.B.), craig.mello@umassmed.edu (C.C.M.)
DOI 10.1016/j.molcel.2008.06.002

SUMMARY

In metazoans, Piwi-related Argonaute proteins have been linked to germline maintenance, and to a class of germline-enriched small RNAs termed piRNAs. Here we show that an abundant class of 21 nucleotide small RNAs (21U-RNAs) are expressed in the *C. elegans* germline, interact with the *C. elegans* Piwi family member PRG-1, and depend on PRG-1 activity for their accumulation. The PRG-1 protein is expressed throughout development and localizes to nuage-like structures called P granules. Although 21U-RNA loci share a conserved upstream sequence motif, the mature 21U-RNAs are not conserved and, with few exceptions, fail to exhibit complementarity or evidence for direct regulation of other expressed sequences. Our findings demonstrate that 21U-RNAs are the piRNAs of *C. elegans* and link this class of small RNAs and their associated Piwi Argonaute to the maintenance of temperature-dependent fertility.

INTRODUCTION

Diverse organisms utilize sequence-specific gene regulatory pathways that share features with RNA interference (RNAi). The effector complex in all RNAi-related pathways consists of a single-stranded small RNA, and a member of the AGO protein family, which binds small-RNA termini, leaving internal nucleotides accessible for base-pairing interactions with target sequences. In canonical RNAi pathways, double-stranded RNA (dsRNA) is processed by members of the Dicer family of multifunctional ribonucleases into 21–24 nucleotide (nt) short interfering RNAs (siRNAs) that interact with and guide AGO proteins to complementary target sequences in the cell (reviewed in Hutvagner and Simard, 2007).

Most animals have an additional AGO subfamily called Piwi. *C. elegans* has two *Piwi-*related *g*enes (named *prg-1* and *prg-2)* that, like Piwi family members from a number of animal species, have been implicated in germline maintenance and fertility (reviewed in Klattenhoff and Theurkauf, 2008). Two classes of *Pi*wi-interacting *RNAs* (piRNAs) have been identified, including (1) repeat-associated piRNAs (originally annotated as rasiRNAs) that appear to target transposons, and (2) a second, more mysterious class of piRNAs with no known targets (Lin, 2007). The latter class of piRNAs is extremely abundant in small-RNA fractions isolated from pachytene-stage mouse spermatocytes: over 80,000 distinct species are derived from large genomic clusters of up to 200 kb (Aravin et al., 2006; Grivna et al., 2006; Girard et al., 2006; Lau et al., 2006). These clusters exhibit a marked strand asymmetry, as though the piRNAs within a region are all processed from one large transcript or two divergent transcripts.

Studies in *C. elegans* have identified several classes of endogenously expressed small RNAs (Ambros et al., 2003; Ruby et al., 2006). However, which, if any, of these represent piRNAs has yet to be determined. One class of small RNAs, termed 21U-RNAs, shares several characteristics with the piRNAs of flies and mammals, including an overwhelming bias for a 5′ uracil, a 5′ monophosphate, and a 3′ end that is modified and resistant to periodate degradation (Ruby et al., 2006; Ohara et al., 2007; Saito et al., 2007; Horwich et al., 2007; Kirino and Mourelatos, 2007). However, 21U-RNAs are shorter than piRNAs in flies and mammals, and their genomic organization is very different, with 21U-RNAs deriving from what appear to be thousands of individual, autonomously expressed loci broadly scattered in two large regions of one chromosome.

Here we show that 21U-RNAs are expressed in the germline and that their accumulation depends on the wild-type activity of PRG-1. We show that PRG-1 localizes to germline P granules

and that 21U-RNAs coimmunoprecipitate with PRG-1 from worm lysates. Our analysis identifies many additional 21U-RNAs, bringing the total number of 21U-RNA loci to 15,722, and confirms the expression of many 21U-RNA loci previously predicted based only on the presence of an upstream sequence motif. Like the abundant pachytene piRNAs found in mammals, 21U-RNAs encode remarkable sequence diversity and yet lack obvious targets. Although we identify one example of a transposon-directed 21U-RNA, our findings suggest that piRNA complexes of worms, charged with the remarkable sequence diversity encoded by 21U-RNAs, are likely to provide other essential germline functions.

RESULTS

### Identification of Over 15,000 Unique 21U-RNA Species in *C. elegans*

We used Solexa sequencing technology (Seo et al., 2004) to generate 29,112,356 small-RNA cDNA reads that perfectly matched the *C. elegans* genome. Among these we identified 971,981 reads from 15,458 unique loci with properties similar to previously defined 21U-RNA loci (Ruby et al., 2006). These reads matched 95.1% of the 5454 previously sequenced 21U-RNAs and 78.3% of the 10,644 previously predicted 21U-RNAs (Ruby et al., 2006) and brought the total number of unique experimentally confirmed 21U-RNA loci to 15,722.

A common characteristic of 21U-RNA loci is the presence of an upstream sequence motif (Figure 1A; Ruby et al., 2006). As previously observed, RNA species 21 nt in length could be separated into two distinct sets based on the motif scores of their genomic loci (Figure 1B). Species with a high motif score also tended to exhibit the other essential features, including 21 nt length and 5′-U nucleotide, that together define the 21U-RNA class (see Figures S1A–S1C available online).

21U-RNAs with strong upstream motif matches were concentrated in two broad regions along chromosome IV (Figure 1C; Ruby et al., 2006). Supporting the potential importance of this motif in 21U-RNA biogenesis, the motif score strongly correlated with the magnitude of 21U-RNA expression, as indicated by the number of sequenced reads in our data sets (Figure 1D). Despite the presence of many high-scoring 21U-RNA motifs in orthologous regions of the *C. briggsae* genome, the 21U-RNA sequences themselves were not conserved. Even in rare cases in which the core of the upstream motif was perfectly aligned to a high-scoring motif within a syntenic region of the *C. briggsae* genome (Blanchette et al., 2004), the sequence of the consequent 21U-RNA was essentially nonconserved (Figure 1E). Only approximately 6% of the 21U-RNA loci and/or motifs were unambiguously aligned within syntenic regions in *C. briggsae.* In these few cases, this was often due to overlap with annotated coding exons, which rarely contain 21U-RNAs (Figure S1D). The only portion of the 21U-RNA flanking regions with elevated conservation frequencies above background was the 8 nt core of the upstream motif (Figure S1E).
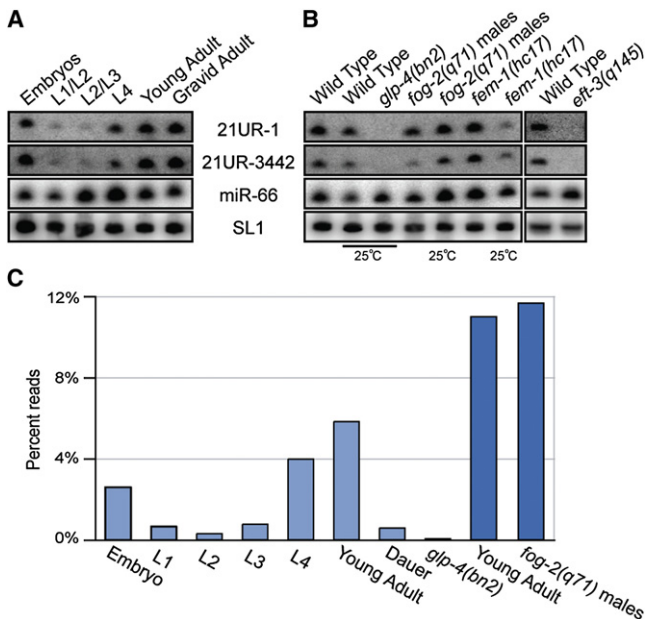
21U-RNAs Are Expressed in the *C. elegans* Germline

The developmental dynamics of 21U-RNA expression were examined by northern blot analysis using probes specific for
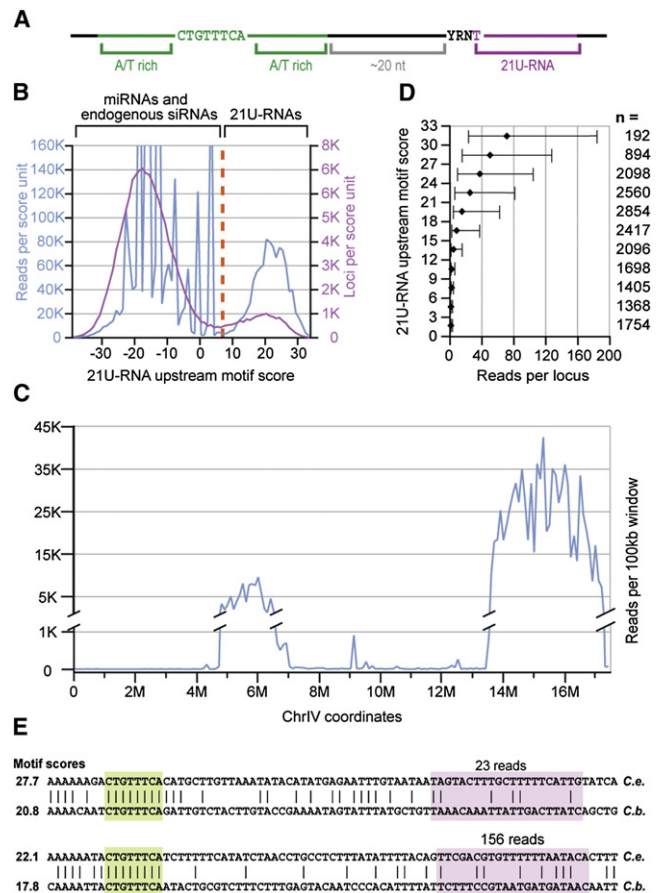
Figure 1. 21U-RNAs Can Be Distinguished from Other RNA Species by Their Lengths and Upstream Motif Matches

(A) A schematic representation of the 21U-RNA upstream motif as described previously (Ruby et al., 2006).

(B) The number of 21 nt RNA reads (blue) or unique loci (pink) corresponding to each upstream motif score (rounded to the nearest unit). A score cut-off of 7 (orange) defined the 21U-RNA population.

(C) The distribution of 21U-RNA reads across chromosome IV. Normalized read counts were summed for each nonoverlapping 100 kb bin (blue).

(D) Correlation between the upstream motif score and the magnitude of 21U-RNA expression. For each three-bit bin of motif scores, the number of reads was determined for every experimentally identified 21U-RNA locus. The median read number is plotted, and the 25th and 75th percentiles are indicated (error bars), as is the number of loci in each bin.

(E) Two 21U-RNA loci whose core upstream motifs are aligned (Blanchette et al., 2004). The core motif (green) and 21U-RNA loci (pink) are highlighted. The *C. briggsae* 21U-RNA was annotated based on the highest-scoring 5′ end corresponding to the conserved core motif. The number of reads from *C. elegans* is indicated, as is the motif score for each 21U-RNA ortholog.

21U-RNA-1 and 21U-RNA-3442. Both small RNAs were expressed at low levels from the L1 to L3 stage, began to accumulate to high levels during the L4 stage, and reached maximal expression in the young adult and gravid adult stages (Figure 2A). This pattern of expression correlated with the proliferation of the germline and was consistent with a germline origin. Both RNAs were expressed at approximately equal levels in male- or female-enriched populations (Figure 2B) but were absent in

Figure 2. 21U-RNAs Are Expressed in the *C. elegans* Germline

(A) RNA isolated from synchronized wild-type populations at the indicated developmental stages analyzed on a northern blot, successively probing for two 21U-RNAs, a miRNA, or a loading control (the SL1 precursor).

(B) RNA isolated from wild-type worms, compared to that obtained from mutant strains *glp-4(bn2)* and *eft-3(q145)*, which lack a germline; *fog-2(q71)*, a male-only population; and *fem-1(hc17)*, which lack sperm, analyzed as in (A).

(C) The expression profile for the bulk population of 21U-RNAs as determined by large-scale sequencing. Plotted for each library is the percent of reads that represented 21U-RNAs. Some libraries were prepared for sequencing starting with Rnl2(1-249) ligase (light blue), and others were prepared starting with T4 RNA ligase 1 (dark blue; see Experimental Procedures).

RNA samples prepared from germline-deficient *glp-4(bn2)* and *eft-3(q145)* mutant populations (Figure 2B). Finally, both small RNAs were present in embryos (Figure 2A), which may reflect maternal and/or paternal loading.

High-throughput sequencing indicated that the developmental expression profile for the entire class of 21U-RNAs was indistinguishable from that of 21U-RNA-1 and 21U-RNA-3442 (Figure 2C). The number of sequenced reads for each 21U-RNA species increased dramatically in late larval and adult stages. Furthermore, the number of reads was reduced (130-fold), from 5.8% to just 0.04% of total reads, in animals lacking a germline (Figure 2C). Adult hermaphrodites switch to an exclusively female mode of gametogenesis and store only 200 to 300 mature sperm. The relative abundance of various individual 21U-RNA species was comparable between male and adult hermaphrodite populations, suggesting that very similar 21U-RNA populations are present in germlines undergoing oogenesis and spermatogenesis.

PRG-1 Is Expressed in the Germline and Required for 21U-RNA Accumulation

To examine whether the accumulation of 21U-RNA-1 and 21U-RNA-3442 was dependent on known components of the RNAi

machinery, we systematically examined RNA prepared from mutant strains lacking specific components of the RNAi pathway. The accumulation of 21U-RNAs did not require the wild-type activities of any of the previously described RNAi pathway components, including DCR-1 (Figure 3A, left, and Figure S2).

To determine if accumulation of 21U-RNAs is dependent on any AGO proteins, we also analyzed mutant strains representing all of the *C. elegans* AGO family members, including several multiple mutant strains. Only *prg-1* mutants lacked 21U-RNA-1 and 21U-RNA-3442 (Figure 3A, right, and data not shown). Strains mutant for *prg-2*, a nearly identical homolog of *prg-1*, did not exhibit defects in 21U-RNA expression (Figure 3A, right). We observed no defects in miRNA expression. However, we did note two 21U-RNAs that appear to have been misannotated as miRNAs (see Supplemental Results). Moreover, *prg-1* mutants exhibited a wild-type RNAi response to foreign dsRNA (data not shown). These findings suggested that *prg-1* was defective specifically in the 21U-RNA pathway.

Consistent with the genetic requirement of *prg-1* for 21U-RNA accumulation, the stage-specific expression of PRG-1 protein was coincident with that of 21U-RNA-1 and 21U-RNA-3442. PRG-1 levels were reduced in L1/L2 and L2/L3 worms when compared with L4 worms, as well as young and gravid adults (Figure 3B). As observed for 21U-RNAs, we could also detect the PRG-1 protein in embryo extracts, and we were unable to detect PRG-1 in the *glp-4(bn2)* mutant strain, suggesting that this protein is expressed in the germline. PRG-1 was also present in protein extracts from both female- and male-enriched populations. Curiously, the expression of *prg-1* was reduced in wild-type worms cultured at 25°C (Figure 3B). Analysis of the expression of the *prg-1/prg-2* mRNA by real-time PCR revealed an expression pattern similar to that observed for the PRG-1 protein. The only exception observed was in the embryonic stage (Figure 3B). Although we could detect a high level of the PRG-1 protein in embryos, the mRNA was almost undetectable, supporting the idea that PRG-1 complexes in embryos are parentally derived.

In wild-type worms, we observed a striking localization of PRG-1 in the cytoplasm and in prominent cytoplasmic structures in germ cells at nearly all stages of germline development. In both hermaphrodites and males, PRG-1 formed perinuclear foci in both the mitotic and meiotic zones of the germline (Figures 3C and 3D). In mature oocytes the staining persisted, but PRG-1 foci lost their perinuclear association and became dispersed in the cytoplasm (Figure 3C and data not shown). In males, all PRG-1 staining disappeared abruptly as spermatids matured (Figure 3D). The pattern of PRG-1 localization, including its localization during embryogenesis (Figures 3E and 3F), resembled that of P granules, which are components of the *C. elegans* germline cytoplasm, or nuage (Strome and Wood, 1982; Strome, 2005). Indeed, the localization of PRG-1 perfectly overlapped, throughout development, the localization of the previously described P granule component, PGL-1 (Kawasaki et al., 1998; Figure 3G; and data not shown).

21U-RNAs Depend on and Interact Physically with PRG-1

To determine whether PRG-1 is required more broadly for 21U-RNA accumulation, we performed high-throughput sequencing
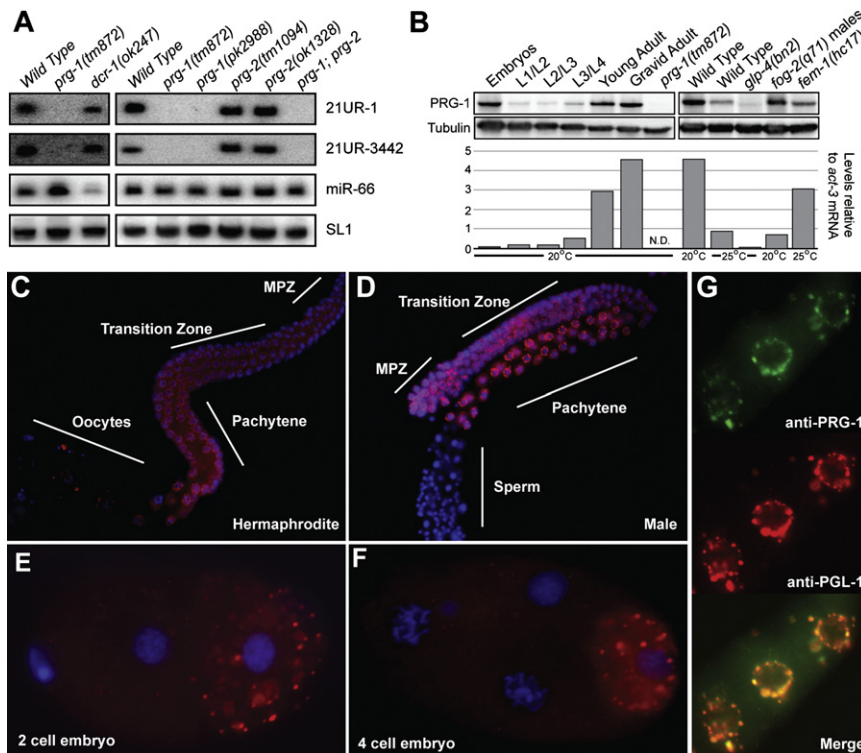
Figure 3. PRG-1 Protein Is Expressed in the Germline and Required for 21U-RNA Accumulation

(A) Northern blot analysis of 21U-RNA-1, 21U-RNA-3442, and miR-66 expression in wild-type and the indicated homozygous strains. The double mutant was *prg-1(tm872); prg-2(tm1094)*. The SL1 precursor served as a loading control.

(B) The PRG-1 developmental expression profile. Protein lysates generated from wild-type populations at distinct developmental stages were analyzed using a western blot (top left), as were protein lysates from wild-type worms and from the mutant strains examined in Figure 2B (top right). Tubulin served as a loading control. Expression of *prg-1/prg-2* mRNA was analyzed by quantitative real-time PCR, using actin (*act-3*) mRNA as the normalization standard (bottom panel).

(C–F) PRG-1 immunofluorescence (red) and DNA DAPI staining (blue) in dissected gonad arms from an adult hermaphrodite (C) and male (D), a two-cell embryo (E), and a four-cell embryo (F). In (C) and (D) the mitotic (MPZ) and meiotic zones (transition zone plus pachytene) are indicated, as are the proximal zones containing oocytes and sperm (respectively).

(G) Dual immunofluorescence analysis of three oocytes in the proximal arm of a wild-type hermaphrodite gonad stained for PRG-1 and PGL-1 as indicated. Yellow represents overlap in the merged image (bottom panel).

analysis on small-RNA populations prepared from *prg-1* mutant animals and from wild-type animals reared at 20°C. For wild-type animals approximately 11% of the 1,789,450 genome-matching reads corresponded to the 21U-RNAs, whereas for *prg-1* mutant animals less than 0.05% of the 1,774,442 genome-matching reads corresponded to 21U-RNAs (Figure 4A). This dramatic reduction in 21U-RNAs resembled that observed in animals lacking a germline altogether (Figure 4B). However, *prg-1* animals maintained at 20°C were fertile and exhibited nearly wild-type levels of another class of germline-enriched small RNAs, the endogenous siRNAs (Figure 4C). These findings indicate that *prg-1* is required for the accumulation of the entire 21U-RNA class of small RNAs.

To examine whether the 21U-RNAs physically interact with PRG-1, we immunoprecipitated the PRG-1 protein complex along with associated RNA. Both 21U-RNA-1 and 21U-RNA-3442 coprecipitated with the PRG-1 immune complex but not with precipitates recovered using preimmune serum (Figure 4D). Small-RNA species that did not require PRG-1 activity for accumulation, such as miR-66, were not detected in PRG-1 immunoprecipitates (Figure 4D). In contrast, we found that ALG-1/ALG-2 AGO-associated immune complex contained miR-66 but not 21U-RNA-1 or 21U-RNA-3442 (Figure 4D).

Biochemical analysis of small RNAs recovered in the PRG-1 IP complex demonstrated a strong bias for small RNAs with 5′ U (>91%) compared to the total input population, which was enriched for 5′ G (>70%; Figure 4E). Similarly, deep sequencing of small-RNA libraries prepared from the IP sample demonstrated a dramatic enrichment for 21 nt RNAs with 5′ U in the

PRG-1 complex (Figure 4F). In addition, 21mers with high-scoring motif matches were dramatically enriched in the IP sample (Figure 4G) and mapped comprehensively across the previously described 21U-RNA clusters on chromosome IV (Figure 4H). No other RNA species was significantly enriched in the PRG-1 IP. The above observations suggest that PRG-1 specifically binds 21U-RNAs to form a complex important for germline function and fertility.

prg-1 Mutants Exhibit a Broad Spectrum of Germline Defects

A previous study demonstrated that RNAi targeting both *prg-1* and *prg-2* leads to reduced fertility (Cox et al., 1998). Our examination of the phenotypic contributions of recently identified probable null alleles revealed that most, if not all, of the germline defects result from the absence of *prg-1*. For example, *prg-2* mutants exhibited wild-type brood sizes at both 20°C and 25°C (Figure 5A) as well as normal numbers of morphologically wild-type germ cells (compare Figures 5B and 5C). In contrast, *prg-1* mutants exhibited dramatically reduced fertility at both temperatures (Figure 5A). Consistent with this phenotype, two different *prg-1* mutant strains and a *prg-1; prg-2* double mutant strain all exhibited a significant reduction in the total number of germ nuclei populating the adult gonad (Figures 5D–5F). The numbers of germ nuclei were reduced in each zone but were most dramatically reduced in the mitotic zone in these mutants. The reduction in germ cell numbers was observed at all temperatures, and thus does not by itself explain the sterility of *prg-1* mutants at 25°C.
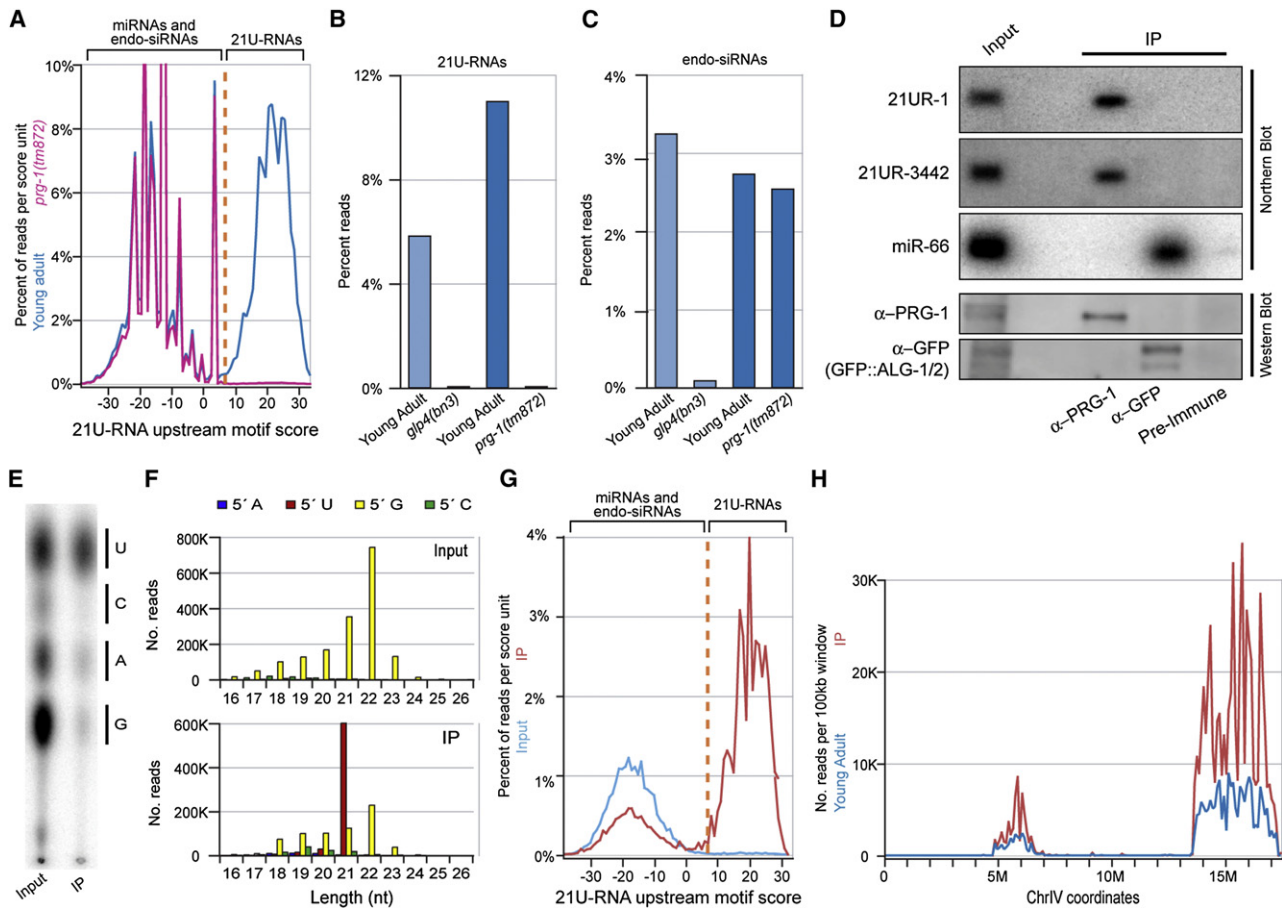
Figure 4. PRG-1 Interacts with and Is Required for the Accumulation of All 21U-RNAs

(A) The percentage of 21 nt RNA reads from wild-type young adults (blue) and *prg-1(tm872)* young adult (pink) corresponding to each upstream motif score (rounded to the nearest unit). A score cutoff of 7 (orange) defined the 21U-RNA population.

(B) Severe depletion of 21U-RNAs in *glp-4(bn2)* and *prg-1(tm872)* mutant worms. Plotted for each library is the fraction of reads corresponding to 21U-RNAs, with bars colored as in Figure 2C.

(C) Severe depletion of endogenous siRNAs in *glp-4(bn2)* but not *prg-1(tm872)* mutant worms. Plotted for each library is the fraction of reads with 5′ G nucleotides and complete antisense overlap with coding exons (Ambros et al., 2003; Ruby et al., 2006), with bars colored as in Figure 2C.

(D) Immunoprecipitation (IP) analysis of small RNAs in PRG-1 and GFP::ALG1/2 complexes. Immunoprecipitations were performed on lysates prepared from an otherwise wild-type transgenic strain carrying GFP-tagged ALG-1 and ALG-2. The top panels show a northern blot successively probed for the indicated small RNAs. The lower panels show western blots probed as indicated.

(E) Biochemical analysis of the first nucleotide of the small-RNA population that coimmunoprecipitated with the PRG-1 protein (IP). Bars show where the single nucleotides migrate in this thin-layer-chromatography system.

(F) The length and 5′ nucleotide distribution of reads from the input (top) and PRG-1 co-IP (bottom) libraries. To prevent underrepresentation of endogenous siRNAs, which usually begin with a 5′ triphosphate, these libraries were constructed using a protocol that does not require a 5′ monophosphate.

(G) The percentage of 21 nt RNA reads from the input (blue) and PRG-1 co-IP (red) libraries at each upstream motif score, plotted as in (A).

(H) The mapping of 21U-RNA reads from the PRG-1 co-IP library (red) versus the young adult wild-type library prepared starting with T4 RNA ligase 1 (see Experimental Procedures; blue). Reads were classified as 21U-RNAs by their motif scores, and normalized read counts were summed for each nonoverlapping 100 kb bin.

Although *prg-1* mutants exhibit temperature-dependent sterility, they do not appear to encode thermo-labile products. Rather, both alleles examined in this study are likely to represent null mutations (Yigit et al., 2006; Cuppen et al., 2007; Figure S3A). As expected for null mutants, the PRG-1 protein was either absent or truncated in these mutant strains at all temperatures (Figure S3B). Furthermore, the 21U-RNA depletion associated with *prg-1* mutants was observed at all temperatures examined, including the semipermissive temperatures of 15°C and 20°C.

These findings suggest that, in addition to their role in maintaining proper germ-cell numbers at all temperatures, PRG-1/21U-RNA complexes may function at higher temperatures to facilitate an otherwise temperature-dependent germline process required for normal fertility.

Temperature-shift experiments demonstrated that the temperature-sensitive period of *prg-1* mutants occurs during the adult stage. The fertility of animals shifted down from 25°C as young adults was substantially rescued, to an average of 40
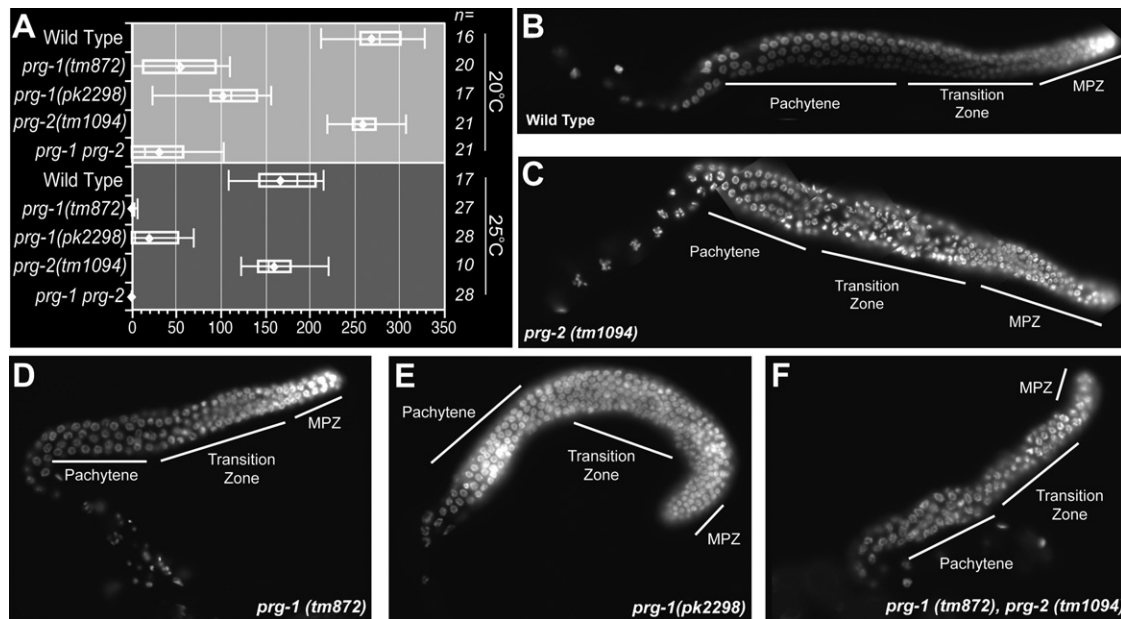
Figure 5. PRG-1 Exhibits a Broad Spectrum of Germline Defects

(A) Brood size analysis of *prg-1* and *prg-2* mutant strains. The brood size of "n" individual animals for each strain was determined at 20°C and 25°C. Left and right lines represent the highest and lowest values, respectively. Left and right ends of each box represent the 75th and 25th percentile, respectively; the diamond represents the average brood size; and the vertical line inside the box represents the median value.

(B–F) DAPI staining of excised gonads from wild-type, *prg-1*, and *prg-2* strains (as indicated). Gonadal zones are indicated as in Figure 3.

progeny (n = 10). Conversely, maintaining animals at 15°C during the L1 to adult stage, when the germline is proliferating most rapidly, did not significantly rescue the fertility defect. These results suggest that the germ cells produced in *prg-1* null mutant animals (that entirely lack PRG-1 protein expression) are deficient in a process important for their functionality at elevated temperature.

To examine the relative contribution of defects in sperm versus oocytes to the reduced fertility of *prg-1* mutants, mutant hermaphrodites raised at 25°C were mated to wild-type males. The temperature-dependent sterility of *prg-1* was partially rescued, as the average number of *prg-1* progeny produced by animals reared at 25°C was 3 (n = 10), but this number increased to 19 (n = 10) when *prg-1* mutants were mated with wild-type males. These findings suggest that the fertility defects of *prg-1* hermaphrodites stem, in part, from defects in the production and/or functionality of both the male and female gametes.

In summary, *prg-1* mutants exhibit dramatically reduced germ-cell numbers at all temperatures, and the gametes produced are markedly more sensitive to temperature than are those of wild-type animals. For example, at 25°C wild-type animals produce ~200 progeny, about two-thirds of the brood size observed at 20°C, while *prg-1* mutants produce an average brood size of only 3 progeny at 25°C, less than one-tenth the brood size of 40 observed at 20°C. This reduction in brood size at higher temperature correlates with a reduction in the number of embryos observed, consistent with the idea that ovulation or fertilization are impaired at higher temperature.

prg-1 Mutants Exhibit Surprisingly Subtle Changes in Gene Expression

On chromosome IV hundreds of protein-encoding genes are interspersed with intergenic and intronic 21U-RNA loci over genomic regions that are millions of base pairs in length. Therefore, tiling arrays were used to profile changes in gene expression to determine whether the absence of 21U-RNAs in *prg-1* mutants might cause significant perturbations of gene expression either on this autosome or elsewhere. We found that *prg-1* and wild-type animals have broadly similar patterns of gene expression. Notably, genes located near 21U-RNA loci, including genes located within and around the major clusters of 21U-RNA loci on chromosome IV, were not significantly altered in their expression (Figure 6A). Among 88 groups of developmentally coregulated genes, also referred to as gene "mountains" (Kim et al., 2001), 66 were essentially unchanged between the wild-type and *prg-1* strains (Figure 6B). Among the 16 mountains with decreased expression in *prg-1* mutants were several mountains with germline functions such as cell division and oogenesis. Among the six mountains with increased expression was one containing spermatogenesis-related genes.

In *C. elegans* a large class of RdRP-derived endogenous siRNAs (endo-siRNAs) target transposons and repetitive sequences as well as numerous protein-encoding genes (Ambros et al., 2003; Ruby et al., 2006; W.G. and D.C., unpublished data). Although PRG-1 does not appear to interact directly with small RNAs of this type (Figure 6C and Tables S2 and S3), we wondered whether 21U-RNAs might be linked, perhaps indirectly, to changes in the patterns of endo-siRNA expression. In many

instances, changes in endo-siRNA levels correlated inversely with changes in gene expression from the corresponding interval (Figure 6D and Table S4). However, the regions with significant changes in endo-siRNA levels were not correlated with regions containing 21U-RNAs or sequences with extended sequence similarity to 21U-RNAs.

One curious exception to this finding was the transposon Tc3, within which resides a single 21U-RNA. Found in all 22 Tc3 genomic loci, 21U-RNA-15703 overlaps the 3′ inverted repeat (IR) downstream of, and in the same orientation as, the transposase gene (Figure 6E). This sequence was identified three times among two million reads in our small-RNA library prepared from the PRG-1 immune complex, an apparent enrichment when compared to only 12 reads in over thirty million from the remaining non-IP-associated data set. Examination of the endo-siRNA profile across a representative Tc3 element revealed two types of endo-siRNA reads. The first were antisense to the transposase gene and were unaffected in *prg-1(tm872)* mutants (Figure 6F). The second were directed, with a marked strand asymmetry, toward the Tc3 IR regions and were severely depleted in *prg-1(tm872)* mutants (Figure 6F). Neither the IR-directed nor the transposase-directed siRNAs exhibited coimmunoprecipitation with PRG-1 (Figure 6G). Although the numbers of endo-siRNAs targeting the transposase gene were not significantly reduced in *prg-1*, we nevertheless observed a 3- to 4-fold upregulation of the Tc3 transposase mRNA (Figure 6H). Upregulation of the transposon mRNA, as well as a greater than 100-fold increase in Tc3 transposition frequency, were also observed for two different *prg-1* mutant alleles in a parallel study (Das et al., 2008 [this issue of *Molecular Cell*]; see Discussion).

DISCUSSION

AGO-protein/small-RNA complexes mediate biological activities that fall into the two broad categories of genomic surveillance and gene regulation. Several studies suggest that a metazoan-specific branch of the AGO family, called the Piwi AGOs, have become specialized to provide surveillance functions required for germline maintenance in animals (reviewed in Aravin et al., 2007). *C. elegans* contains one of the largest and best studied families of AGO proteins. Yet, beyond a general requirement for fertility (Yigit et al., 2006), the function of *C. elegans* Piwi-related AGOs and the nature of their small-RNA cofactors had not been explored. We have shown that PRG-1, a Piwi subfamily AGO, interacts with 21U-RNAs, which are encoded by over 15 thousand genomic loci broadly clustered in two regions of chromosome IV. These findings link this unusual class of small RNAs to an RNAi-related pathway and suggest that PRG-1 and 21U-RNAs form an RNP complex required for proper germline development. The sequence repertoire of 21U-RNAs appears to be more diverse than expected by chance, and, with the exception of Tc3 discussed below, obvious sequence-specific targets for 21U-RNAs are not found in the *C. elegans* genome.

piRNAs in Worms, Flies, and Mammals
Piwi AGOs bind small RNAs (piRNAs) with the following characteristics: a Dicer-independent biogenesis, a 5′ end with a monophosphate and a strong bias for Uracil, and a 3′ end that is modified and resistant to periodate degradation (reviewed in Klattenhoff and Theurkauf, 2008). The *C. elegans* 21U-RNAs share these characteristics but also exhibit several other unique properties (Ruby et al., 2006). Perhaps the most remarkable distinction is that 21U-RNAs originate from thousands of loci that frequently share a common upstream motif and are clustered in two large regions of one autosome. Within these two large regions of two million and four million base pairs, respectively, the 21U-RNA loci are interspersed on both strands and rarely overlap with each other, repeat elements, or coding regions. Instead they localize to introns and intergenic regions within these chromosomal regions at an average density of one 21U-RNA locus every 200–300 bp.

In other organisms, piRNAs lack discernable upstream motifs and are often found in much smaller clusters dispersed on all chromosomes. In flies a subgroup of piRNAs, originally termed repeat-associated siRNAs (rasiRNAs), are derived primarily from within repeats and transposons and appear to target transposons for silencing (Brennecke et al., 2007; Gunawardane et al., 2007; Saito et al., 2006). Furthermore, unlike 21U-RNAs, repeat-associated piRNAs derived from opposite strands frequently overlap.

In mammals, two types of piRNA clusters have been identified based on their temporal expression during spermatogenesis. Similar to *Drosophila* rasiRNAs, piRNAs expressed prior to meiotic pachytene in mice are derived from repeat- and transposon-rich clusters. These rasi-like piRNAs interact with the MILI AGO, which is expressed in the same developmental stages (Aravin et al., 2007). During pachytene a second type of piRNA becomes abundant, which is derived from clusters that differ from both 21U-RNA clusters and rasiRNA clusters. These pachytene piRNA clusters span tens of thousands of bases—the length of a typical pre-mRNA transcript. Within these clusters the piRNAs exhibit remarkable strand bias, as though all the piRNAs within a region are processed from a single RNA-Polymerase II transcript or from two divergent transcripts (Aravin et al., 2006; Girard et al., 2006; Grivna et al., 2006; Lau et al., 2006). In contrast, neighboring 21U-RNA loci, even those within the same intron of an annotated gene, appear to have autonomous biogenesis, each with their own 5′ motif and deriving from the opposite strand about as often as from the same strand.

Despite these striking differences, mammalian pachytene piRNAs are similar to 21U-RNAs in one very intriguing way. Both types of small RNA encode tremendous sequence diversity and yet seem to lack obvious targets. In general, 21U-RNAs do not match repeat sequences or protein coding genes with a frequency any higher than that expected by chance.

Piwi-AGO Complexes Exhibit a Conserved Localization in Germline Nuage
We have shown that the PRG-1 protein localizes to the germline nuage, called P granules, in *C. elegans*. In other animals, Piwi AGOs show similar localization. In both *Drosophila* (AGO3 and Aubergine) and zebrafish (Ziwi), Piwi proteins localize to perinuclear nuage structures (Brennecke et al., 2007; Houwing et al., 2007). A third Piwi protein from *Drosophila*, Piwi itself, exhibits a more complex distribution, localizing to the nuclei of both germ cells and somatic cells (Brennecke et al., 2007; Cox
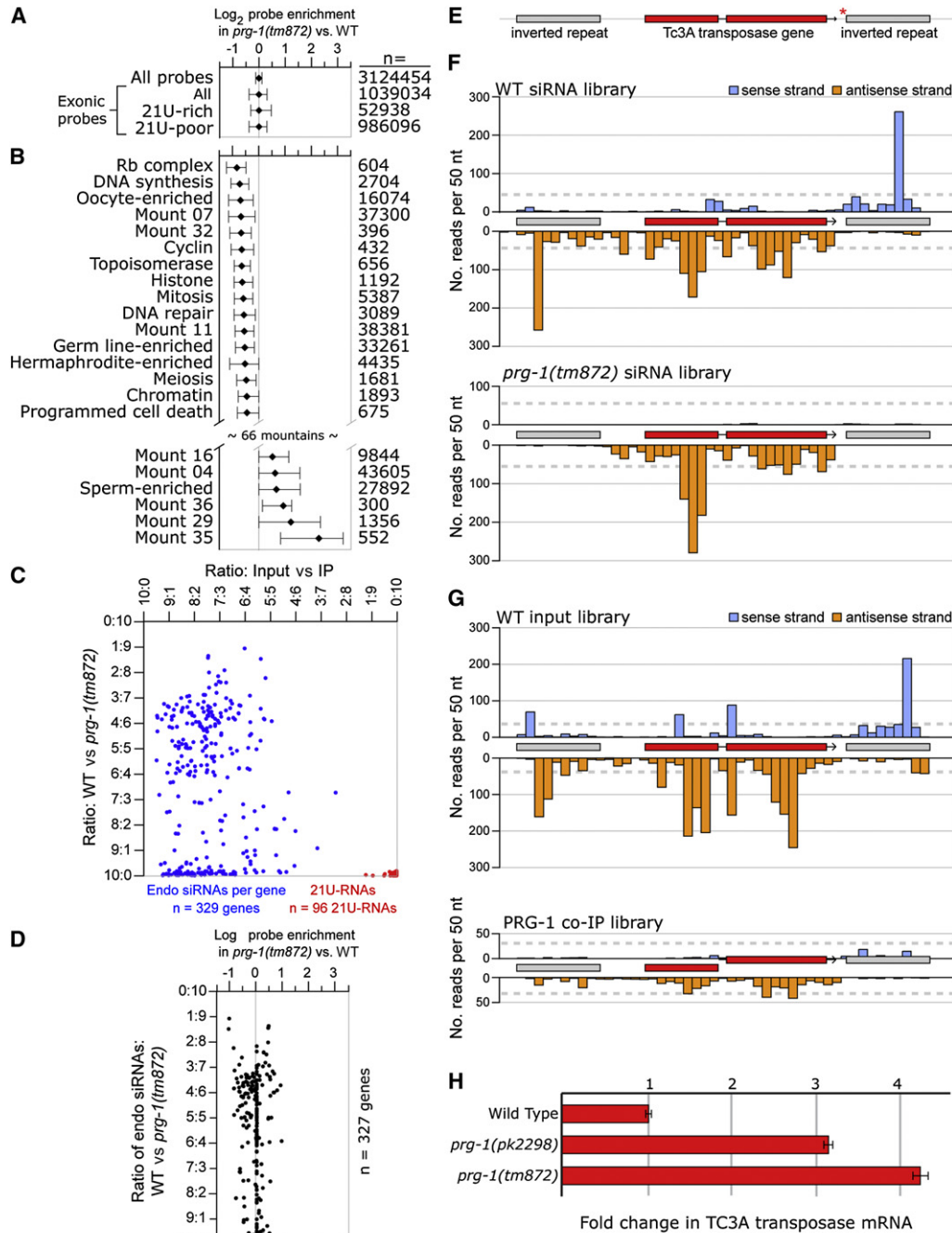
Figure 6. *prg-1* Mutants Exhibit Surprisingly Subtle Changes in Gene Expression

(A) Gene expression was not preferentially affected in the 21U-rich portions of the *C. elegans* genome. For each of the indicated probe sets, median values are shown with error bars indicating 25th and 75th percentiles and "n" indicating the number of probes.

(B) The overall expression of some gene mountains was significantly altered in the *prg-1* (*tm872*) mutant. All probes overlapping the exons of all genes from each mountain (Kim et al., 2001) were considered, and median log-fold changes were plotted as in (A) for those mountains changing by ≥ 0.4 log$_2$ units.

(C) 21U-RNA depletion in the *prg-1(tm872)* mutant and enrichment in the PRG-1 co-IP. The x axis indicates the ratio of read frequencies between the input versus PRG-1 co-IP libraries described in Figures 4F–4H. The y axis indicates the ratio of antisense read frequencies between the wild-type and *prg-1(tm872)* mutant siRNA-enriched libraries (made using a protocol that does not require a 5′ monophosphate and therefore captures endogenous siRNAs beginning with a 5′ tri-phosphate). Each blue dot indicates the antisense read count for one gene whose wild-type siRNA-enriched read count is ≥ 500. Each red dot indicates the read count for a 21U-RNA species with ≥ 200 reads from the young adult wild-type library prepared starting with T4 RNA ligase 1 (see Experimental Procedures) and at least one read between the two libraries of each plot axis.
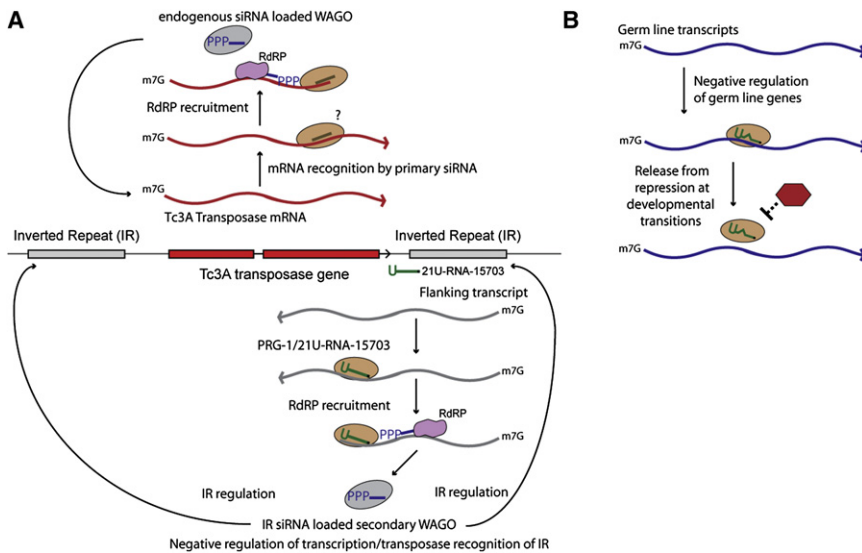
Figure 7. Models for 21U-RNA Function

(A) Regulation of TC3 inverted repeats by PRG-1/21U-RNA-15703.

(B) Regulation of germline transcripts by imperfect base paring.

(Tijsterman et al., 2002). Surprisingly, the silencing of a single transposon family, Tc3, appears to depend on both WAGO family members (Vastenhouw et al., 2003) and on *prg-1* (Das et al., 2008).

We found a single 21U-RNA, 21U-RNA-15703, that mapped to Tc3. This 21U-RNA appeared enriched among small RNAs recovered from the PRG-1 immune complex but was located downstream of the transposase 3′UTR in the sense orientation and thus could not directly silence the transposase mRNA. Interestingly, 21U-RNA-15703 was located just upstream of a series of siRNAs associated with the Tc3 inverted repeats (IR). The production of IR-associated siRNAs depended on *prg-1* but also required the activities of two RdRPs and of an AGO in the WAGO clade (data not shown).

The production of the PRG-1-dependent IR-associated siRNAs could be explained by a two-step model similar to one previously described for RDE-1-directed silencing in *C. elegans* (Yigit et al., 2006; Sijen et al., 2007; Pak and Fire, 2007). If a PRG-1 complex containing 21U-RNA-15703 were to cleave a target RNA that extended into Tc3 from the downstream genomic region (Figure 7A), it could create a template for the RdRP-dependent synthesis of the secondary IR-associated siRNAs. How the loss of these IR-associated siRNAs might lead to activation of Tc3 in *prg-1* mutants remains unclear. Perhaps their loss leads to alterations in chromatin structure in the IRs or to changes in the expression of IR-associated regulatory transcripts. Such changes could explain the 3- to 4-fold increase in transposase mRNA levels observed by qRT-PCR and might also render the IR genomic regions more accessible for transposase-directed endonucleolytic cleavage. The notion that PRG-1 may serve as an upstream AGO capable of triggering secondary siRNA production has implications for how other 21U-RNAs may function and could explain how loss of an exceptionally low-abundance 21U-RNA could cause the 100-fold increase in transposition of Tc3 (Das et al., 2008).

et al., 2000). In mice, the localization of Miwi and Mili has been analyzed, and, although their expression peaks at different times, both are cytoplasmic proteins present in developing spermatids but absent in mature sperm (Deng and Lin, 2002; Kuramochi-Miyagawa et al., 2004).

A striking feature of PRG-1 localization was its presence in P granules throughout development. In germline stem cells and developing gametes of *C. elegans*, P granules are localized in a perinuclear pattern and are often found in apposition to nuclear pores (Pitt et al., 2000). They are thought to function in the sorting and storage of messages involved in gametogenesis and in subsequent parentally programmed zygotic development (Strome, 2005). In the fertilized egg and early embryo, the P granules dissociate from the nuclear periphery and are distributed in the cytoplasm. In the male germline, P granules are present in dividing stem cells as well as meiotic spermatocytes but rapidly disappear as the spermatids mature. Finally, similar to other organisms where piRNA expression correlates tightly with the expression of their Piwi-class AGO binding partners (Aravin et al., 2006; Girard et al., 2006; Houwing et al., 2007), the expression of 21U-RNAs closely correlated with the expression of PRG-1.

A Potential Role for 21U-RNAs in Tc3 Silencing

In *C. elegans*, members of an expanded *worm*-specific *AGO* clade (the WAGOs) are required for the majority of transposon silencing and appear to function with RdRP-derived siRNAs

(D) Changes to mRNAs compared to their corresponding siRNA in the *prg-1(tm872)* mutants. Each point indicates a gene with ≥10 array probes and ≥500 antisense reads from the WT siRNA-enriched library overlapping annotated exons. The x axis is as in (A). The y axis is as in (C).

(E) A schematic view of a full-length Tc3 transposon showing the inverted repeats (gray) and Tc3A transposase gene (red). The position of 21U-RNA-15703 is indicated with a red asterisk.

(F) Density of reads mapping to the sense (blue) and antisense (orange) strands of the Tc3 element from (E). Reads per 50 nt window are plotted for the wild-type (top) and *prg-1(tm872)* mutant (bottom) siRNA-enriched libraries. Read counts are not normalized to the number of genomic matches. Dashed gray lines indicate 0.002% of each library.

(G) Density of reads mapping to the sense (blue) and antisense (orange) strands of the Tc3 element from (E). Reads per 50 nt window are shown from the input (top) and PRG-1 co-IP (bottom) libraries. Read counts are not normalized to the number of genomic matches. Dashed gray lines indicate 0.002% of each library.

(H) Expression of the *TC3A* mRNA. Primers recognizing *TC3A* mRNA were used in quantitative RT-PCR on mRNA generated from worms with the indicated genotypes, using actin *(act-3)* mRNA as the normalization standard.

A Conserved Function for piRNA Complexes in Maintaining Pluripotency

Despite differences in their expression and the types of clusters from which they derive, our findings suggest that the overwhelming majority of 21U-RNAs and the abundant pachytene piRNAs of mammals share some intriguing similarities. Perhaps most notably, they share the confounding feature that, with few exceptions, they lack recognizable targets upon which they might specifically act. Although a number of genes exhibit changes in expression in *prg-1* mutants, these changes could easily reflect alterations that arise indirectly. A parallel study has suggested that spermatogenesis-related gene expression is downregulated in *prg-1* mutant males (Wang and Reinke, 2008). Conversely, our studies revealed an apparent upregulation of several spermatogenesis-related genes in *prg-1* mutant hermaphrodites. However, in these instances, unlike the Tc3 example, there is no direct evidence linking specific 21U-RNAs to the regulated genes, therefore it seems probable that these apparent discrepancies reflect indirect consequences of developmental defects and changes in germ-cell number that occur in the *prg-1* mutant gonads. Overall, our analyses suggest that there is no correlation between genes whose expression is altered in *prg-1* mutants and the proximity of those genes to 21U-RNA loci.

One possible model to explain this paradox is to imagine that PRG-1/21U-RNA complexes may base-pair imperfectly with targets. A precedent for this already exists with animal miRNAs and most of their targets, for which pairing to miRNA seed nucleotides 2–8 is often sufficient for target recognition (Grimson et al., 2007). However, if similar partial matches were sufficient for piRNA-mediated regulation, then the entire transcriptome could potentially be placed under 21U-RNA-directed regulation. Perhaps 21U-RNAs act collectively, through partial sequence matches, to negatively regulate gene expression broadly. For example, germline-expressed mRNAs recognized by 21U-RNA/PRG-1 complexes could be stored in the cytoplasm (perhaps within P granules) until a secondary factor releases repression (Figure 7B). Such a mechanism would require the maintenance of sequence diversity within the 21U-RNA family as a whole, rather than conservation of specific 21U-RNA sequences.

Out of more than 15,000 different 21U-RNAs encoded in *C. elegans*, only one transposon-directed 21U-RNA was identified, strongly suggesting that transposon silencing is not the only function mediated by this ancient metazoan-specific group of AGOs. It is interesting to note that many mammals, including humans, have, at great apparent cost to their fitness (Werdelin and Nilsonne, 1999), derived morphological adaptations that place the male germline external to the body cavity. Perhaps this adaptation is necessary to facilitate the same temperature-sensitive process in gametogenesis that is also facilitated in part by PRG-1.

EXPERIMENTAL PROCEDURES

Worm Strains

The Bristol strain N2 was used as the standard wild-type strain. Alleles used in this study are listed below, grouped by chromosome: LGI: *glp-4(bn2)*, *prg-1(tm872)*, *prg-1(pk2298)*, *rde-3(ne3364)*, *ego-1(om71)*, *rrf-1(ok589)*, *rrf-2(pk2040)*; LGII: *rrf-3(pk1426)*; LGIII: *dcr-1(ok247)*, *rde-4(ne299)*, *mut-7(ne311)*, *eft-3(q145)*, *qC1[nels(myo2::avr-15, rol-6, unc-22(RNAi))]*; LGIV: *fem-1(hc17)*, *prg-2(ok1328)*, *prg-2 (tm1094)*; LGV: *fog-2(q71)*. AGO deletions described in Yigit et al. (2006) were also assayed for levels of 21U-RNA-1 and 21U-RNA-3442. *C. elegans* culture and genetics were as described in Brenner (1974).

Antibody Generation

Anaspec generated and purified the PRG-1 antibody in rabbits using the following peptides: RGSGSNNSGGKDQKYL and RQQGQSKTGSSGQPQKC.

Biochemistry and Molecular Biology

Protein and RNA purifications were performed as described in Hutvagner et al. (2004) and Duchaine et al. (2006), respectively. Antibodies used in this study are as follows: (1) monoclonal antibody anti-AFP 3E6 (Qbiogene), (2) an affinity-purified polyclonal anti-PRG-1 antibody, (3) HRP-conjugated secondary antibody (Jackson Immunoresearch), (4) anti-tubulin (Accurate Chemical). Northern blot analysis was performed as in Duchaine et al. (2006). A more detailed description can be found in the Supplemental Experimental Procedures.

Quantitative Real-Time PCR

Real-time PCR was performed using Superscript III Reverse Transcriptase (Invitrogen) and Applied Biosystems SYBR Green PCR Master mix according to the supplier's instructions. Primer sequences are available upon request.

Immunostaining and Microscopy

Gonads were prepared for indirect immunofluorescence as in Pasierbek et al. (2001) and incubated with primary antibody (K76 [Kawasaki et al., 1998] and the anti-PRG-1 antibodies described above) overnight at 4°C. Cy-3 anti-mouse IgM, and FITC or TRITC anti-rabbit secondary antibodies (Jackson Immunoresearch), were used to detect K76 anti-PGL-1 and anti-PRG-1, respectively. Slides were mounted in Vectashield (Vector Labs) with DAPI. All images were collected using a Hamamatsu Orca-ER digital camera mounted on a Zeiss Axioplan 2 microscope and with Openlab software.

Small-RNA Cloning

Small endogenous *C. elegans* RNAs from embryos, five distinct larval stages (L1, L2, L3, L4, and dauer), mixed-stage animals, young adults from *glp-4(bn2)*, *prg-1(tm872)*, *fog-2(q71)* mutant backgrounds, and wild-type control worms were prepared for sequencing using a protocol derived from Lau et al. (2001). Libraries generated from wild-type and *prg-1(tm872)* were constructed as described by W.G. and D.C. (unpublished data). To generate small-RNA libraries from PRG-1 immunocomplexes, PRG-1 IPs were performed on 70 mg of total wild-type protein as described in Duchaine et al. (2006). For comparison, total RNA was extracted from a fraction of worms equivalent to that used for the PRG-1 IPs. These small-RNA libraries were constructed using a method that does not require a 5′ monophosphate (Ambros et al., 2003. PCR products generated for all the samples described above were sequenced on a Solexa sequencing platform (Illumina, Inc.) (Seo et al., 2004). Detailed description of the cloning protocols, as well as data analysis, can be found in the Supplemental Experimental Procedures.

Biochemical Analysis of 5′ Nucleotide

Small RNAs in the 18–26 nt range, obtained from total RNA and the RNA fraction that coimmunoprecipitated with PRG-1, were gel purified, treated with Calf Intestinal Alkaline Phosphatase (NEB) in the presence of 1 U of Super RNase Inhibitor (Ambion), and labeled at the 5′ end with T4 Polynucleotide Kinase in the presence of γATP. The 5′ end-labeled RNAs were gel purified and incubated with nuclease P1 (USBiological). Samples were spotted on a TLC plate developed with 0.5 M lithium chloride.

Tiling Microarray Procedures

Total RNA was extracted as described above and prepared using the Ribo-Pure total RNA isolation kit (Ambion). Labeling reactions were performed following the manufacturer's protocols with the GeneChip WT Double-Stranded cDNA Synthesis Kit (Affymetrix), GeneChip Sample Cleanup Module (Affymetrix), and the GeneChip WT Double Stranded DNA Terminal Labeling Kit (Affymetrix). Array hybridization to GeneChip *C. elegans* Tiling 1.0R chips was done using standard Affymetrix protocols and reagents. Signal values for each array

probe were calculated using Affymetrix Tiling Analysis Software 1.1.2 (bandwidth: 30; intensities: PM/MM) with three replicates of *prg-1(tm872)* experimental data sets and three control wild-type. Probe overlap with annotations was assessed using the Affymetrix-provided ce4 coordinate, which indicates the genomic position matching the center of the array probe.

ACCESSION NUMBERS

All RNA sequences extracted from Illumina reads as described were deposited in the Gene Expression Omnibus with the following accession number: GSE11738. Included under this accession number are the following data sets: developmental time-course/mixed stage, 5′ monophosphate-dependent; *prg-1(tm872)* and *fog-2(q71)* mutant analysis, 5′ monophosphate-dependent; *prg-1(tm872)* mutant analysis, 5′ monophosphate-independent; and the PRG-1 co-IP analysis. 21U-RNA sequences are provided as a supplemental Fasta-formatted text file (Table S1). Tools for scoring 21U-RNA loci trained using data from Ruby et al. (2006) and applied here are available for anonymous download at http://web.wi.mit.edu/bartel/pub/.

SUPPLEMENTAL DATA

The Supplemental Data include Supplemental Results, Supplemental Experimental Procedures, three figures, and four tables and can be found with this article online at http://www.molecule.org/cgi/content/full/31/1/67/DC1/.

ACKNOWLEDGMENTS

REFERENCES

Ambros, V., Lee, R.C., Lavanway, A., Williams, P.T., and Jewell, D. (2003). MicroRNAs and other tiny endogenous RNAs in C. elegans. Curr. Biol. *13*, 807–818.

Aravin, A., Gaidatzis, D., Pfeffer, S., Lagos-Quintana, M., Landgraf, P., Iovino, N., Morris, P., Brownstein, M.J., Kuramochi-Miyagawa, S., Nakano, T., et al. (2006). A novel class of small RNAs bind to MILI protein in mouse testes. Nature *442*, 203–207.

Aravin, A.A., Sachidanandam, R., Girard, A., Fejes-Toth, K., and Hannon, G.J. (2007). Developmentally regulated piRNA clusters implicate MILI in transposon control. Science *316*, 744–747.

Blanchette, M., Kent, W.J., Riemer, C., Elnitski, L., Smit, A.F., Roskin, K.M., Baertsch, R., Rosenbloom, K., Clawson, H., Green, E.D., et al. (2004). Aligning multiple genomic sequences with the threaded blockset aligner. Genome Res. *14*, 708–715.

Brennecke, J., Aravin, A.A., Stark, A., Dus, M., Kellis, M., Sachidanandam, R., and Hannon, G.J. (2007). Discrete small RNA-generating loci as master regulators of transposon activity in Drosophila. Cell *128*, 1089–1103.

Brenner, S. (1974). The genetics of Caenorhabditis elegans. Genetics *77*, 71–94.

Cox, D.N., Chao, A., Baker, J., Chang, L., Qiao, D., and Lin, H. (1998). A novel class of evolutionarily conserved genes defined by piwi are essential for stem cell self-renewal. Genes Dev. *12*, 3715–3727.

Cox, D.N., Chao, A., and Lin, H. (2000). piwi encodes a nucleoplasmic factor whose activity modulates the number and division rate of germline stem cells. Development *127*, 503–514.

Cuppen, E., Gort, E., Hazendonk, E., Mudde, J., van de Belt, J., Nijman, I.J., Guryev, V., and Plasterk, R.H. (2007). Efficient target-selected mutagenesis in Caenorhabditis elegans: toward a knockout for every gene. Genome Res. *17*, 649–658.

Das, P.P., Bagijn, M.P., Goldstein, L.D., Woolford, J.R., Lehrbach, N.J., Sapetschnig, A., Buhecha, H.R., Gilchrist, M.J., Howe, K.L., Stark, R., et al. (2008). Piwi and piRNAs act upstream of an endogenous siRNA pathway to suppress Tc3 transposon mobility in the *Caenorhabditis elegans* germline. Mol. Cell *31*, this issue, 79–90.

Deng, W., and Lin, H. (2002). miwi, a murine homolog of piwi, encodes a cytoplasmic protein essential for spermatogenesis. Dev. Cell *2*, 819–830.

Duchaine, T.F., Wohlschlegel, J.A., Kennedy, S., Bei, Y., Conte, D.J., Pang, K., Brownell, D.R., Harding, S., Mitani, S., Ruvkun, G., Yates, J.R., III, and Mello, C.C. (2006). Functional proteomics reveals the biochemical niche of *C. elegans* DCR-1 in multiple small-RNA-mediated pathways. Cell *124*, 343–354.

Girard, A., Sachidanandam, R., Hannon, G.J., and Carmell, M.A. (2006). A germline-specific class of small RNAs binds mammalian Piwi proteins. Nature *442*, 199–202.

Grimson, A., Farh, K.K., Johnston, W.K., Garrett-Engele, P., Lim, L.P., and Bartel, D.P. (2007). MicroRNA targeting specificity in mammals: determinants beyond seed pairing. Mol. Cell *27*, 91–105.

Grivna, S.T., Beyret, E., Wang, Z., and Lin, H. (2006). A novel class of small RNAs in mouse spermatogenic cells. Genes Dev. *20*, 1709–1714.

Gunawardane, L.S., Saito, K., Nishida, K.M., Miyoshi, K., Kawamura, Y., Nagami, T., Siomi, H., and Siomi, M.C. (2007). A slicer-mediated mechanism for repeat-associated siRNA 5′ end formation in Drosophila. Science *315*, 1587–1590.

Horwich, M.D., Li, C., Matranga, C., Vagin, V., Farley, G., Wang, P., and Zamore, P.D. (2007). The *Drosophila* RNA methyltransferase, DmHen1, modifies germline piRNAs and single-stranded siRNAs in RISC. Curr. Biol. *17*, 1265–1272.

Houwing, S., Kamminga, L.M., Berezikov, E., Cronembold, D., Girard, A., van den Elst, H., Filippov, D.V., Blaser, H., Raz, E., Moens, C.B., et al. (2007). A role for Piwi and piRNAs in germ cell maintenance and transposon silencing in Zebrafish. Cell *129*, 69–82.

Hutvagner, G., and Simard, M.J. (2007). Argonaute proteins: key players in RNA silencing. Nat. Rev. Mol. Cell Biol. *9*, 22–32.

Hutvagner, G., Simard, M.J., Mello, C.C., and Zamore, P.D. (2004). Sequence-specific inhibition of small RNA function. PLoS Biol. *2*, E98. 10.1371/journal.pbio.0020098.

Kawasaki, I., Shim, Y.H., Kirchner, J., Kaminker, J., Wood, W.B., and Strome, S. (1998). PGL-1, a predicted RNA-binding component of germ granules, is essential for fertility in *C. elegans*. Cell *94*, 635–645.

Kim, S.K., Lund, J., Kiraly, M., Duke, K., Jiang, M., Stuart, J.M., Eizinger, A., Wylie, B.N., and Davidson, G.S. (2001). A gene expression map for Caenorhabditis elegans. Science *293*, 2087–2092.

Kirino, Y., and Mourelatos, Z. (2007). The mouse homolog of HEN1 is a potential methylase for Piwi-interacting RNAs. RNA *13*, 1397–1401.

Klattenhoff, C., and Theurkauf, W. (2008). Biogenesis and germline functions of piRNAs. Development *135*, 3–9.

Kuramochi-Miyagawa, S., Kimura, T., Ijiri, T.W., Isobe, T., Asada, N., Fujita, Y., Ikawa, M., Iwai, N., Okabe, M., Deng, W., et al. (2004). Mili, a mammalian member of piwi family gene, is essential for spermatogenesis. Development *131*, 839–849.

Lau, N.C., Lim, L.P., Weinstein, E.G., and Bartel, D.P. (2001). An abundant class of tiny RNAs with probable regulatory roles in Caenorhabditis elegans. Science *294*, 858–862.

Lau, N.C., Seto, A.G., Kim, J., Kuramochi-Miyagawa, S., Nakano, T., Bartel, D.P., and Kingston, R.E. (2006). Characterization of the piRNA complex from rat testes. Science *313*, 363–367.

Lin, H. (2007). piRNAs in the germ line. Science *316*, 397.

Ohara, T., Sakaguchi, Y., Suzuki, T., Ueda, H., Miyauchi, K., and Suzuki, T. (2007). The 3′ termini of mouse Piwi-interacting RNAs are 2′-O-methylated. Nat. Struct. Mol. Biol. *14*, 349–350.

Pak, J., and Fire, A. (2007). Distinct populations of primary and secondary effectors during RNAi in C. elegans. Science *315*, 241–244.

Pasierbek, P., Jantsch, M., Melcher, M., Schleiffer, A., Schweizer, D., and Loidl, J. (2001). A Caenorhabditis elegans cohesion protein with functions in meiotic chromosome pairing and disjunction. Genes Dev. *15*, 1349–1360.

Pitt, J.N., Schisa, J.A., and Priess, J.R. (2000). P granules in the germ cells of Caenorhabditis elegans adults are associated with clusters of nuclear pores and contain RNA. Dev. Biol. *219*, 315–333.

Ruby, J.G., Jan, C., Player, C., Axtell, M.J., Lee, W., Nusbaum, C., Ge, H., and Bartel, D.P. (2006). Large-scale sequencing reveals 21U-RNAs and additional microRNAs and endogenous siRNAs in *C. elegans*. Cell *127*, 1193–1207.

Saito, K., Nishida, K.M., Mori, T., Kawamura, Y., Miyoshi, K., Nagami, T., Siomi, H., and Siomi, M.C. (2006). Specific association of Piwi with rasiRNAs derived from retrotransposon and heterochromatic regions in the Drosophila genome. Genes Dev. *20*, 2214–2222.

Saito, K., Sakaguchi, Y., Suzuki, T., Suzuki, T., Siomi, H., and Siomi, M.C. (2007). Pimet, the Drosophila homolog of HEN1, mediates 2′-O-methylation of Piwi- interacting RNAs at their 3′ ends. Genes Dev. *21*, 1603–1608.

Seo, T.S., Bai, X., Ruparel, H., Li, Z., Turro, N.J., and Ju, J. (2004). Photo-cleavable fluorescent nucleotides for DNA sequencing on a chip constructed by site-specific coupling chemistry. Proc. Natl. Acad. Sci. USA *101*, 5488–5493.

Sijen, T., Steiner, F.A., Thijssen, K.L., and Plasterk, R.H. (2007). Secondary siRNAs result from unprimed RNA synthesis and form a distinct class. Science *315*, 244–247.

Strome, S. (2005). Specification of the germ line. In WormBook, The *C. elegans* Research Community, ed. 10.1895/wormbook.1.9.1, http://www.wormbook.org.

Strome, S., and Wood, W.B. (1982). Immunofluorescence visualization of germ-line-specific cytoplasmic granules in embryos, larvae, and adults of Caenorhabditis elegans. Proc. Natl. Acad. Sci. USA *79*, 1558–1562.

Tijsterman, M., Okihara, K.L., Thijssen, K., and Plasterk, R.H. (2002). PPW-1, a PAZ/PIWI protein required for efficient germline RNAi, is defective in a natural isolate of *C. elegans*. Curr. Biol. *12*, 1535–1540.

Vastenhouw, N.L., Fischer, S.E., Robert, V.J., Thijssen, K.L., Fraser, A.G., Kamath, R.S., Ahringer, J., and Plasterk, R.H. (2003). A genome-wide screen identifies 27 genes involved in transposon silencing in *C. elegans*. Curr. Biol. *13*, 1311–1316.

Wang, G., and Reinke, V. (2008). A *C. elegans* Piwi, PRG-1, regulates 21U-RNAs during spermatogenesis. Curr. Biol. *18,* in press. Published online May 22, 2008. 10.1016/j.cub.2008.05.009.

Werdelin, L., and Nilsonne, A. (1999). The evolution of the scrotum and testicular descent in mammals: a phylogenetic view. J. Theor. Biol. *196*, 61–72.

Yigit, E., Batista, P.J., Bei, Y., Pang, K.M., Chen, C.C., Tolia, N.H., Joshua-Tor, L., Mitani, S., Simard, M.J., and Mello, C.C. (2006). Analysis of the *C. elegans* Argonaute family reveals that distinct Argonautes act sequentially during RNAi. Cell *127*, 747–757.